Propagation of Surface Plasmon Polaritons on Semiconductor Gratings

J. Gómez Rivas,* M. Kuttge, P. Haring Bolivar, and H. Kurz
Institut für Halbleitertechnik, RWTH Aachen, Sommerfeldstrasse 24, D-52056 Aachen, Germany

J. A. Sánchez-Gil
Instituto de Estructura de la Materia, Consejo Superior de Investigaciones Científicas, Serrano 121, E-28006 Madrid, Spain
(Received 5 August 2004; published 14 December 2004)

We present time-domain measurements of terahertz surface plasmon polaritons (SPPs) propagating on gratings structured on silicon surfaces. Using single-cycle pulses of terahertz radiation to excite SPPs in a broad frequency range, we observe that the efficient SPPs scattering on the semiconductor periodic structure introduces significant dispersion and modifies the SPPs propagation. A stop gap, or a frequency range where SPPs are Bragg reflected, is formed by the structure. This gap depends strongly on the Si doping density and type. The resonant scattering at the edge of the gap reduces the group velocity by more than a factor of 2. The measurements show a good agreement with our numerical calculations based on the reduced Rayleigh equation.

DOI: 10.1103/PhysRevLett.93.256804 PACS numbers: 73.20.Mf, 42.25.Bs, 42.79.Dj, 78.68.+m

Surface plasmon polaritons (SPPs) are electromagnetic waves trapped on a metal-dielectric interface and coupled to the oscillation of free charge carriers [1]. The two-dimensional nature of SPPs and the strong electromagnetic field at the interface are the reasons why SPPs are used for the spectroscopy of surfaces and of thin films deposited on metals. Surface plasmon polaritons are also responsible for fascinating phenomena such as surface enhanced Raman scattering [2] and the extraordinary transmission of light through nanoholes [3]. The possibility of guiding electromagnetic waves with SPPs beyond the diffraction limit has resulted in an unprecedented interest in the field of surface plasmon photonics or plasmonics [4]. The propagation of SPPs can be controlled by structuring the metal surface. The interference of scattered SPPs gives rise to the inhibition of the propagation at certain directions and the enhancement at others. The propagation of optical SPPs through single defects [5,6], gratings [7–9], 2D photonic crystals [10–13], and stripes [14] has been recently investigated experimentally, and simple plasmonic circuits have been demonstrated [15]. A detailed knowledge of the SPP dynamics on complex structures will be fundamental for the development of plasmonic devices. In spite of this important aspect, continuous wave excitation has been used in most of the previous experiments. Only recently, the dynamics of SPPs propagating in photonic crystals was observed by interferometric correlation measurements [13].

In this Letter, we present the first terahertz time-domain measurements of broadband SPP pulses propagating on complex structures, i.e., gratings of grooves. With our measuring technique we readily obtain the phase of the transmitted pulse and we can easily reconstruct the SPPs dispersion relation and calculate the SPPs group velocity. Bragg reflection by the grating gives rise to a stop gap or a frequency range where the transmission of SPPs vanishes. The grating modifies the dispersion relation, and the resonant scattering at the edge of the stop gap slows down the group velocity of SPPs by more than a factor of 2 with respect to the SPPs velocity on a flat surface.

Our gratings are structured in doped silicon instead of metals. The SPP characteristics are determined by the permittivity of the metallic material and of the dielectric. At low frequencies (far infrared, terahertz, and microwaves) metals have a very large complex permittivity, which leads to SPPs weakly confined to the surface [16]. For instance, the decay length into air of SPPs propagating on a gold surface at terahertz frequencies is on the order of centimeters. This very large decay length sets a constraint to most applications in which a strong confinement of SPPs to the surface is required. Furthermore, the scattering of weakly bounded SPPs with surface structures is not efficient [10], limiting the realization of gratings and photonic crystals for low frequency SPPs. This limitation can be overcome by using doped semiconductors [17]. Semiconductors behave at low frequencies as metals in the optical range, thereby making it possible to excite and propagate SPPs on semiconductor-dielectric interfaces. Moreover, the dielectric properties of semiconductors can be modified by varying the carrier density, allowing a much more feasible control of the SPPs propagation.

For the experiments, we use a terahertz time-domain spectrometer [18]. A detailed description of our setup can be found in Ref. [16]. Terahertz pulses are coupled into SPPs which propagate on the sample surface. After some distance, these SPPs are coupled back into free propagating radiation which is detected. For the coupling of the terahertz radiation into SPPs and their coupling back into radiation, we use the aperture method [16]: terahertz pulses are scattered at the small gap of 300 μm defined

by a razor blade and the surface of the sample, and the scattered wave can couple to SPPs. A similar aperture placed a distance of 2 cm from the first one is used to couple back the SPPs into free-space radiation. The gray curve in Fig. 1 shows a typical transient of a SPP. This transient corresponds to a SPP propagating on the flat surface of an n-doped silicon wafer.

We have investigated the propagation of SPPs on the gratings of grooves structured on n-doped silicon with a carrier density of $N \approx 10^{18}$ cm^{-3} and on p-doped silicon with a carrier density of $N \approx 10^{19}$ cm^{-3}. The different free charge carrier densities and mobilities lead to different permittivities of the semiconductor and, as we are going to show, to different SPP characteristics. The gratings have a lattice constant of 442 μm and consist of 30 parallel grooves with a depth of 100 μm and width of 221 μm. These grooves were structured with a programmable wafer dicing saw on commercially available wafers with a diameter of 4 in. A scanning electron microscope image of a piece of one of those gratings is displayed in the inset of Fig. 1.

The black curve in Fig. 1 represents a SPP pulse on the n-doped silicon surface after propagating through the grating. Compared to the reference measurement of SPPs on a flat silicon surface with nominally identical doping (gray curve in Fig. 1), the grating reduces the amplitude of the transmitted pulse and introduces significant dispersion as is evident by the relatively large terahertz signal at long time delays.

To analyze the transmission through the gratings, we calculate the complex Fourier transform of the time-domain signals. This transformation leads to a transmission of the form $T = t(\nu)\exp[i\phi(\nu)]$, where $t(\nu)$ is the spectrally resolved amplitude, $\phi(\nu)$ the phase of the transmitted pulse, and ν the frequency. Defining the transmittance as the power spectrum normalized by the reference, i.e., $t(\nu)^2/t_{\mathrm{ref}}(\nu)^2$, these are plotted in Fig. 2 as open circles. The data of Fig. 2(a) correspond to the transmittance through the grating structured on the n-doped Si wafer, while those of Fig. 2(b) represent the transmittance through the p-doped wafer. Small misalignments in the setup between the reference and the grating measurements are corrected by normalizing the transmittance at low frequencies.

The solid curves in Fig. 2 are numerical results for the transmittance, calculated in the following manner [19]. An impedance boundary condition on a planar surface is imposed to the only nonzero component of the scattered magnetic field (p polarization) in vacuum, expressed as a plane wave expansion, the weight function of which is referred to as the scattering amplitude. The resulting integral equation in k space (reduced Rayleigh equation) is numerically solved for the corresponding scattering amplitude, from which all relevant physical quantities can be retrieved. The reflection and transmission amplitudes are given by the residues of the scattering amplitude at the poles (SPP wave vectors), whereas the angular distribution of scattered power propagating into vacuum is obtained from the scattering amplitude within the radiative region. Such formulation has been employed to theoretically investigate SPP scattering by a single groove or ridge with both continuous wave [20] and pulsed excitations [21]. Except for the fact that absorptive losses are neglected (justified as long as the SPP absorption length exceeds that of the scatterers), the employed scattering formulation is exact within numerical accuracy. However, care has to be taken when relating surface

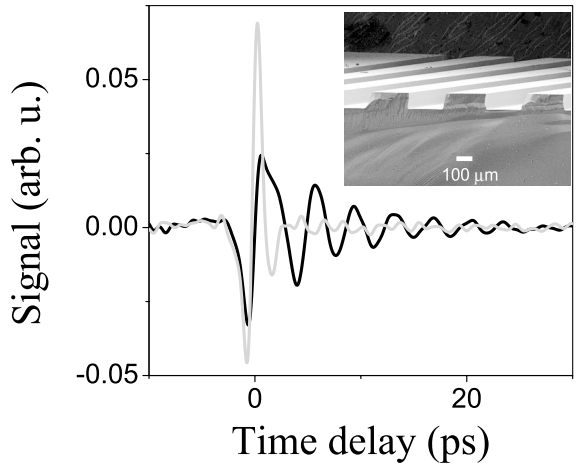

FIG. 1. Terahertz SPP transients. The gray curve corresponds to SPPs propagating on a flat n-doped Si surface with a carrier density of $N \approx 10^{18}$ cm^{-3}. The black curve corresponds to a SPP transient transmitted through a grating of 30 grooves with a lattice constant of 442 μm, groove depth of 100 μm, and groove width of 221 μm structured on a similar Si wafer. Inset: scanning electron microscope image of a SPP grating.

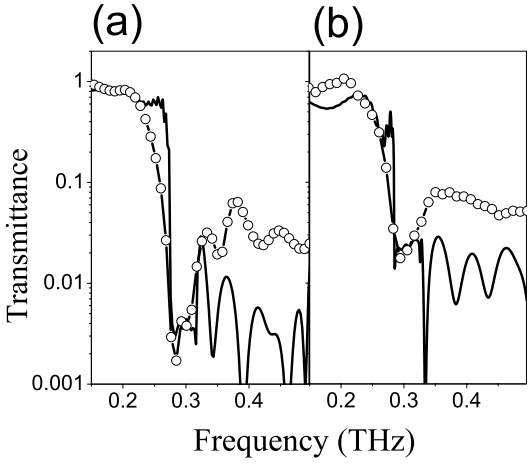

FIG. 2. Transmittance as a function of the frequency of SPPs propagating on gratings of grooves structured on Si wafers. The open circles are measurements and the solid curves numerical calculations. (a) corresponds to a grating structured on n-doped Si, while (b) corresponds to a similar grating structured on p-doped Si.

impedance to actual corrugation [22]; they are assumed to be linearly connected to lowest order in the groove depth and for small skin depth [19].

As can be seen in Fig. 2, there is good agreement between theory and experiments. One should keep in mind that all the parameters in the calculation are known, and therefore there are no fitting variables. For both gratings the SPP transmittance rapidly decreases at $\simeq 0.25$ THz and reaches a minimum at 0.3 THz. This decrease is the result of Bragg scattering: SPPs are Bragg reflected by the grating leading to a decrease of the transmission and the formation of the stop gap. The frequency position of the gap is determined by the periodic structure of the grating, being the same for both gratings. One can observe that the stop gap edge in the calculations is steeper than that in the measurements. The reason for this difference might be that in the calculations the wave front of the SPPs is considered to be plane and incident perpendicular to the grooves axis, while in the experiments SPPs are excited by scattering of the terahertz radiation at the in-coupling aperture with a beam waist size of the order of 1 mm. Although the scattering should be highly anisotropic and the excited SPPs propagate mainly perpendicular to the grating, due to the finite beam waist there will be an spreading of wave vectors incident on the grating which smooths the band edge.

For the same number of grooves, we observe in Fig. 2 that the reduction of the transmittance in the stop gap is more intense for the grating structured on the *n*-doped silicon wafer. This reduction is determined by the different permittivities of either type of doped silicon surfaces. The permittivity of semiconductors in the terahertz range is determined by the carrier density and mobility [23]. The lower dopant density of the *n*-doped wafer and the higher mobility of electrons than that of holes lead to a smaller absolute value of the permittivity in the investigated frequency range. As a consequence of the smaller permittivity, the skin depth and the SPP wave vector are larger, resulting in more efficient stop gaps [24]. In other words, the SPPs on either type of doped Si surface probe the gratings in a different manner, despite having identical structure.

We also observe in Fig. 2 that the transmittance increases at $\simeq 0.325$ THz. However, it does not reach unity again. The reason for the lower than unity transmittance at high frequencies is radiative losses: SPPs become leaky waves (namely, their dispersion relation lies within the light cone) which are partially coupled by the grating into free propagating terahertz radiation, being lost before they reach the out-coupling aperture. The measured high frequency transmittance is larger than expected from the calculations. This discrepancy stems from the fact that in the experiments a small fraction of the SPPs coupled by the grating into free-space radiation slips through the out-coupling aperture and is detected, raising the signal.

The dynamic propagation of the SPPs can be investigated as a function of frequency through the phase of the complex Fourier transform of the time-domain data. The SPP wave number k is directly obtained from the phase difference $\Delta\phi$ between the transmitted and reference pulses

$$k(\nu) = \frac{\Delta\phi}{L} + k_0(\nu), \tag{1}$$

where L is the thickness of the grating and $k_0(\nu)$ is the wave number of SPPs propagating on a flat surface. At low frequencies $k_0(\nu) \simeq \omega/c$, [1] where $\omega = 2\pi\nu$ is the angular frequency and c the speed of light in vacuum. In Fig. 3 we plot with open circles the measured dispersion relation at low frequencies for the SPPs on the *n*-doped Si grating. The theoretical dispersion relation is plotted in the same figure with a solid curve, as obtained from Eq. (1) with $\Delta\phi$ given by the numerically calculated transmission amplitude. For comparison, we have also plotted the dispersion relation of SPPs on a flat surface of *n*-doped Si (dashed curve in Fig. 3). The periodic structure of the grating modifies significantly the dispersion relation. The difference between the measured and calculated dispersion relations can be ascribed to the excitation of SPPs: as mentioned, the aperture excitation generates SPPs propagating mainly perpendicular to the grating. However, there is a spreading of wave vectors given by the scattering characteristics of the aperture, which smooths the stop-band edge and the dispersion relation. In addition, the use in the calculations of a surface impedance that does not exactly reproduce the actual groove profile may account in part for the band edge mismatch.

The SPPs group velocity v_g is defined as $v_g = \frac{L}{\tau_g}$, where L is the grating thickness and τ_g the group time delay. This time delay is related to the phase difference by $\tau_g = \frac{\partial\Delta\phi}{\partial\omega} + \tau_0$, where τ_0 is the group time delay on a flat

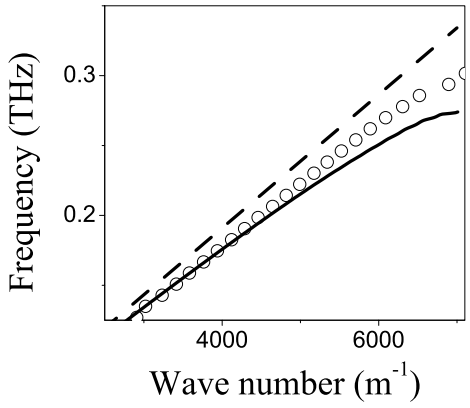

FIG. 3. Dispersion relation of SPPs on a grating of grooves structured on an *n*-doped silicon wafer. The open circles are measurements, while the solid curve is a calculation. The dashed curve represents the dispersion relation of SPPs on a flat Si surface.

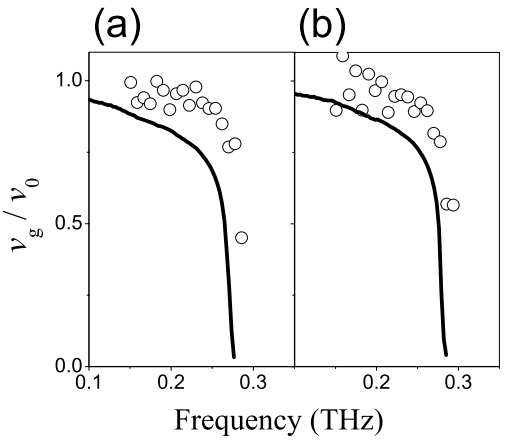

FIG. 4. Group velocity of SPPs on gratings normalized by the velocity of SPPs on flat surfaces. The open circles correspond to measurements, while the solid curves are numerical calculations. (a) corresponds to a grating structured on an *n*-doped Si wafer, while (b) corresponds to a similar grating on a *p*-doped Si wafer.

surface [21]. This experimentally determined group velocity in the low frequency band normalized by the group velocity of SPPs on a flat surface v_0 is plotted in Fig. 4. Figure 4(a) corresponds to the grating structured on *n*-doped Si, and Fig. 4(b) to the grating on the *p*-doped Si wafer. The error in these data, which leads to their scattering and to unphysical values of $v_g > v_0$ at low frequencies, is mainly caused by the numerical derivation of the phase difference. The large dispersion at the edge of the stop gap, due to the resonant scattering of SPPs, reduces the group velocity by approximately a factor of 2 with respect to v_0. The group velocity reduction seems to be more pronounced in the *n*-doped Si grating, although this statement is not conclusive from our measurements. The solid curves in Fig. 4 are the numerical calculations of the group velocities, exhibiting a similar behavior as the measurements. Ideally, one should expect a zero group velocity at the gap edge for an infinite and lossless grating.

In summary, we have investigated the propagation of terahertz SPPs through gratings structured on *n*- and *p*-doped silicon wafers. Doped semiconductors exhibit a behavior at terahertz frequencies similar to that of metals at optical frequencies, thus being an optimal material for the emerging field of low frequency plasmonics. We observe a stop gap for SPPs in both types of gratings and significant dispersion. This dispersion reduces the SPPs group velocity. Low group velocities are required for sensitive spectroscopy and nonlinear applications. Moreover, a detailed knowledge of the dispersion and group velocity of SPPs is of crucial relevance for the development of plasmonic elements and circuits. As we have seen, terahertz time-domain spectroscopy provides this knowledge.

We are indebted to B. Hadam for the scanning electron microscope photographs. We gratefully acknowledge financial support from the European Union through the TMR project Interaction and by the Deutsche Forschungsgemeinschaft. The work of J. A. S. G. was supported in part by the Spanish MEC Grant No. BFM2003-0427. He also acknowledges valuable discussions on the theoretical formulation with A. A. Maradudin under the auspices of the NSF Grant No. INT-0084423.

*Email address: Jaime.Gomez@THz-photonics.com
Electronic address: http://www.THz-photonics.com

[1] H. Raether, *Surface Plasmons on Smooth and Rough Surfaces and on Gratings*, Springer Tracts in Modern Physics Vol. 111 (Springer-Verlag, Berlin, 1988).
[2] F. J. Garcia-Vidal and J. B. Pendry, Phys. Rev. Lett. **77**, 1163 (1996).
[3] T. W. Ebbesen, H. J. Lezec, H. F. Ghaemi, T. Thio, and P. A. Wolff, Nature (London) **391**, 667 (1998).
[4] W. L. Barnes, A. Dereux, and T. W. Ebbesen, Nature (London) **424**, 824 (2003).
[5] I. Smolyaninov, D. L. Mazzoni, and C. C. Davis, Phys. Rev. Lett. **77**, 3877 (1996).
[6] S. Bozhevolnyi and F. A. Pudonin, Phys. Rev. Lett. **78**, 2823 (1997).
[7] S. C. Kitson, W. L. Barnes, G. W. Bradberry, and J. R. Sambles, J. Appl. Phys. **79**, 7383 (1996).
[8] W. L. Barnes, T. W. Preist, S. C. Kitson, and J. R. Sambles, Phys. Rev. B **54**, 6227 (1996).
[9] J. Yoon, G. Lee, S. H. Song, C.-H. Oh, and P.-S. Kim, J. Appl. Phys. **94**, 123 (2003).
[10] W. L. Barnes, S. C. Kitson, T. W. Preist, and J. R. Sambles, J. Opt. Soc. Am. A **14**, 1654 (1997).
[11] I. I. Smolyaninov, W. Atia, and C. C. Davis, Phys. Rev. B **59**, 2454 (1999).
[12] S. I. Bozhevolnyi, J. Erland, K. Leosson, P. M. W. Skovgaard, and J. M. Hvam, Phys. Rev. Lett. **86**, 3008 (2001).
[13] Y.-H. Liau, S. Egusa, and N. F. Scherer, Opt. Lett. **27**, 857 (2002).
[14] J.-C. Weeber, Y. Lacroute, and A. Dereux, Phys. Rev. B **68**, 115401 (2003).
[15] H. Ditlbacher, J. R. Krenn, G. Schider, A. Leitner, and F. R. Aussenegg, Appl. Phys. Lett. **81**, 1762 (2002).
[16] J. Saxler, J. Gómez Rivas, C. Janke, H. P. M. Pellemans, P. Haring Bolivar, and H. Kurz, Phys. Rev. B **69**, 155427 (2004).
[17] J. Gómez Rivas, C. Schotsch, P. Haring Bolivar, and H. Kurz, Phys. Rev. B **68**, 201306 (2003).
[18] D. R. Grischkowsky, S. Keiding, M. van Exter, and C. Fattinger, J. Opt. Soc. Am. B **7**, 2006 (1990).
[19] J. A. Sánchez-Gil and A. A. Maradudin, Phys. Rev. B **60**, 8359 (1999).
[20] J. A. Sánchez-Gil, Appl. Phys. Lett. **73**, 3509 (1998).
[21] J. A. Sánchez-Gil and A. A. Maradudin, Opt. Lett. **28**, 2255 (2003).
[22] A. A. Maradudin, in *Topics in Condensed Matter Physics*, edited by M. P. Das (Nova, New York, 1994).
[23] M. van Exter and D. Grischkowsky, Appl. Phys. Lett. **56**, 1694 (1990).
[24] J. A. Sánchez-Gil and J. Gómez-Rivas (to be published).